Ultrasound in Med. & Biol. Vol. 17, No. 7, pp. 709–714, 1991
Printed in the U.S.A.

0301-5629/91 $3.00 + .00

●*Original Contribution*

THE ULTRASONIC PROPERTIES OF GASTRIC CANCER TISSUES OBTAINED WITH A SCANNING ACOUSTIC MICROSCOPE SYSTEM

YOSHIFUMI SAIJO, MOTONAO TANAKA, HIROAKI OKAWAI and FLOYD DUNN†
Department of Medical Engineering and Cardiology, Research Institute for Chest Diseases and Cancer, Tohoku University, Sendai 980, Japan and †Bioacoustics Research Laboratory, University of Illinois, Urbana, IL 61801, USA

(*Received* 31 *August* 1990; *in final form* 15 *March* 1991)

Abstract—A newly developed scanning acoustic microscope (SAM) system operating in the frequency range of 100–200 MHz has been employed to measure the attenuation and the sound speed of formalin-fixed specimens of five different types of gastric cancer. Signet-ring cell carcinoma specimens exhibit attenuation constant and sound speed values significantly lower than other types of gastric cancer tissues. Tubular adenocarcinoma specimens exhibit a trend toward higher attenuation and sound speed values as the cell type become differentiated. Our measurements and observations suggest that the ultrasonic properties are influenced by cellular arrangement, intercellular junction and intracellular chemical components.

Key Words: **Scanning acoustic microscope, Gastric cancer, Attenuation constant, Sound speed, Ultrasonic tissue characterization.**

INTRODUCTION

A specially developed scanning acoustic microscope (SAM) system has been employed to determine quantitatively the ultrasonic properties of biological tissues (Okawai et al. 1987, 1988). Endoscopic ultrasonography (EUS), which is also undergoing development (DiMango et al. 1980), has observed a five-layered structure of the alimentary tract and submucosal invasions of cancerous tissue not detected by standard endoscopic biopsy. However, EUS cannot be used as yet for the classification of gastric cancer. We report measurements of ultrasonic attenuation and sound speed of five different types of gastric cancer tissues by using the SAM system. We include a discussion of the acoustical properties of gastric cancer tissues.

METHODS

Twenty surgically excised gastric cancer tissue specimens from twenty patients were studied. The specimens were formalin-fixed, paraffin-embedded and sliced in sections approximately 10 μm in thickness by a microtome. The specimens were mounted on glass slides, but were not covered by cover slips for measurement by the SAM system. The paraffin was removed just before the ultrasonic measurement by graded alcohol methods.

The classification of the gastric cancer specimens was done pathologically and found to be papillary adenocarcinoma, well-differentiated tubular adenocarcinoma, moderately-differentiated tubular adenocarcinoma, poorly-differentiated adenocarcinoma and signet-ring cell carcinoma.

The SAM system can display two-dimensional distributions of the attenuation constant and the sound speed at the microscopic level. Figure 1 is a block diagram of the SAM system. The ultrasonic frequency is variable over the range of 100–200 MHz and the beam width is 5 μm (at 200 MHz) to 10 μm (at 100 MHz) at the focal volume. The ultrasonic beam is transmitted for every 4 μm interval over a 2 mm width with the mechanical scanner. The number of sampling points are 480 in one scanning line, and 480 $\times$ 480 points make one frame in 4 s.

Figure 2 is a schematic illustration of the relationship between the ultrasonic beam components and the tissue sample. The detected wave amplitude and phase shift are described by the following relations:

$$L = -(10 \log y^2 - 10 \log y_3^2)$$

$$\phi = \arg(y/y_3)$$

$$y = y_1 + y_2$$

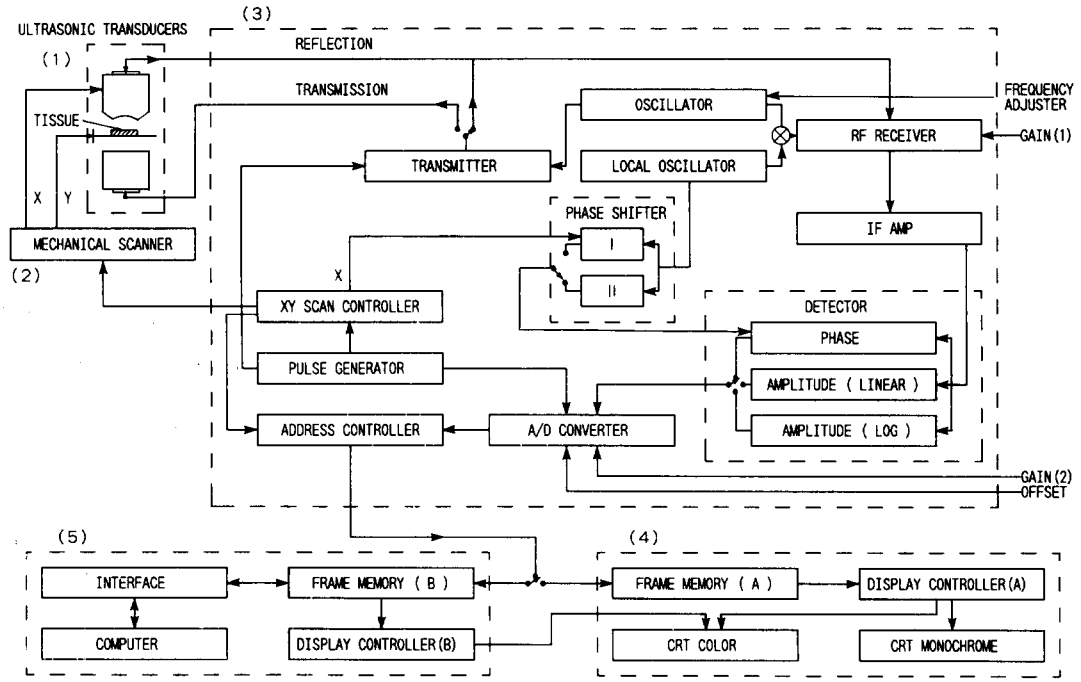

Fig. 1. Block diagram of the scanning acoustic microscope system. (1) Ultrasonic transducers; (2) mechanical scanner; (3) analogue signal processor; (4) display unit; (5) image processor.

where L is the amplitude, ϕ is the phase shift and y_1, y_2, y_3 are the ultrasonic beam components illustrated in Fig. 2.

The original image produced in the analogue signal processor can be displayed in the display unit directly. However, these original data do not have values of attenuation constant or sound speed. Figure 3 is the flow chart showing the processing steps for determining the attenuation constant and the sound speed. The image processor stores the 16 original images; 11 amplitude images in the range 100–200 MHz and five phase images in the range 100–140 MHz. The thickness of the specimen is determined from the frequency characteristics of the amplitude and the phase images (Okawai et al. 1987). The attenuation constant and the sound speed are calculated by the computer using the equations:

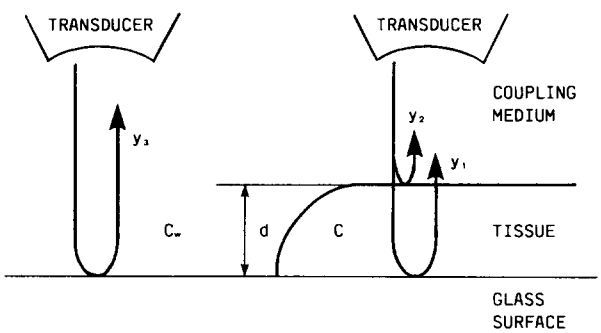

Fig. 2. Schematic illustration of the relationship between the ultrasonic components and the tissue sample. (y_1, y_2, y_3: ultrasonic beam components; C: specimen sound speed; C_w: sound speed of coupling medium; d: thickness of specimen).

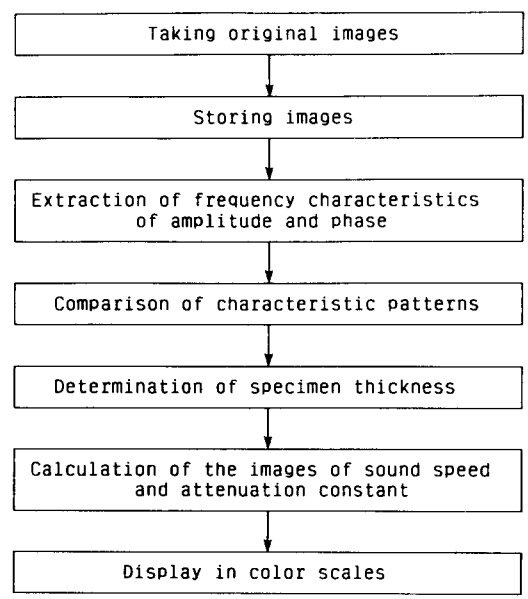

Fig. 3. Flow chart of processing actual values of attenuation constant and sound speed.

Table 1. Relationship between color bar scale and values of attenuation constant and sound speed.

Color bar scale	Attenuation constant (dB/mm/MHz)	Sound speed (m/s)
Red	(≧2.375)	(≧1765)
Magenta	(2.25 ± 0.125)	(1750 ± 15)
Orange	(2.00 ± 0.125)	(1720 ± 15)
Brown	(1.75 ± 0.125)	(1690 ± 15)
Yellow	(1.50 ± 0.125)	(1660 ± 15)
Green	(1.25 ± 0.125)	(1630 ± 15)
Olive green	(1.00 ± 0.125)	(1600 ± 15)
Cyan	(0.75 ± 0.125)	(1570 ± 15)
Royal blue	(0.50 ± 0.125)	(1540 ± 15)
Blue	(0.25 ± 0.125)	(1510 ± 15)
Black	(<0.125)	(<1495)

$$A = L/f/d$$

$$C = (1/C_w - \phi/2\pi fd)^{-1}$$

where A is the attenuation constant, f is the frequency, d is the thickness of specimen, C is the specimen sound speed, C_w is the sound speed of coupling medium and ϕ is the phase shift.

In the ultrasonic frequency range 100–200 MHz, a linear frequency dependency of the attenuation was obtained from consideration of the interference of the sound wave components. In this way, attenuation constant and sound speed were calculated and two-dimensional distributions of these values were displayed on a color monitor. Table 1 shows the relationship between color bar scales and values of attenuation constant and sound speed. Distilled water was used for the coupling medium and the temperature of the coupling medium was maintained between 22–24°C during the measurement procedure.

A neighboring section of the SAM specimen was cut and stained with hematoxylin-eosin (H-E). The region of interest (ROI) for acoustic microscopy was

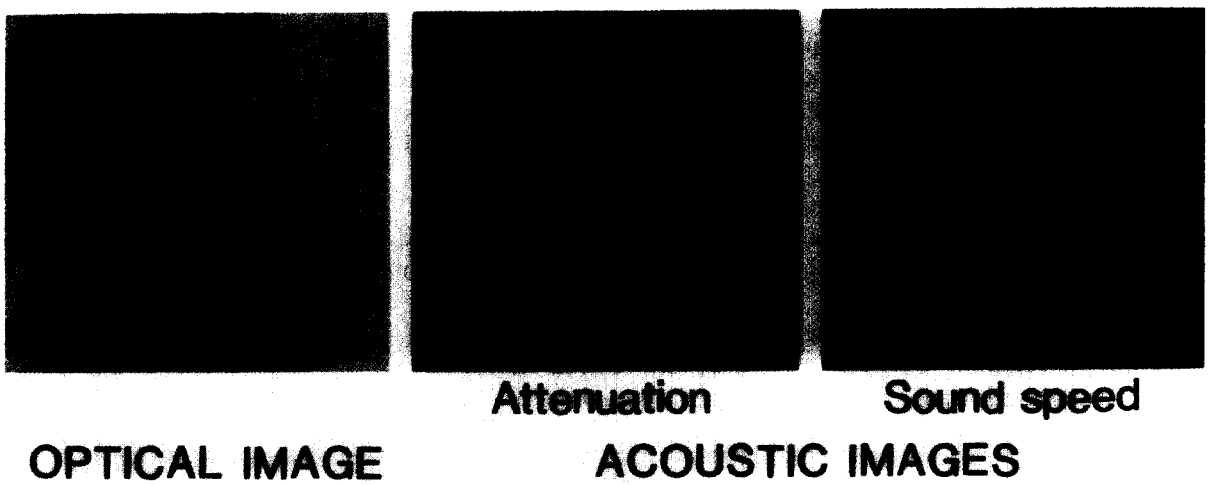

Fig. 4. Optical and acoustic images of well-differentiated tubular adenocarcinoma (×40). The color bar scale of each image relates to values of attenuation constant and sound speed (Table 1).

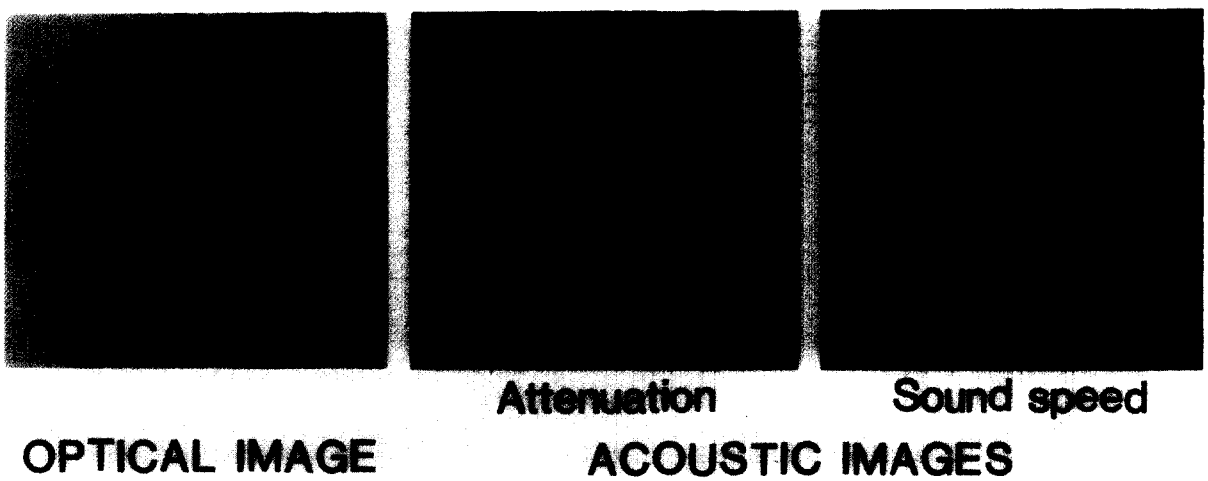

Fig. 5. Optical and acoustic images of signet-ring cell carcinoma (×40). Infiltration of signet-ring cell in the submucosal layer is observed.

determined after observation of the optical microscopic view. Ultrasonic attenuation and sound speed of the ROI were determined in three regions of each specimen and the mean and the standard deviation were calculated by the computer which processed all the data. The attenuation constant and the sound speed were compared among the groups using analysis of variance.

RESULTS

Figure 4 shows the optical and acoustical images (left: attenuation, right: sound speed) of a specimen of well-differentiated tubular adenocarcinoma. The color bar scale of each image relates to values of attenuation constant and sound speed. The figure shows that the attenuation constant varies from 1.0–2.25 dB/mm/MHz and that the sound speed is in the 1600–1750 m/s range in the cancerous lesion. These values are greater than those of normal mucosal tissue. Figure 5 is a signet-ring cell carcinoma specimen. The infiltration of signet-ring cells are seen in the submucosal layer. Both attenuation constant and sound speed were least in this type of gastric cancer; 0.25–0.75 dB/mm/MHz and 1510–1570 m/s, respectively.

Table 2 shows the calculated data for all specimens for each type of gastric cancer and normal mucosa, and Fig. 6 is a graphic illustration of the ranges

Table 2. Calculated data in each type of gastric cancer and normal mucosa. Values are given as mean ± standard deviation. Significant differences between normal mucosa and other gastric cancer tissues are indicated by daggers: $^{\dagger}p < 0.05$; $^{\ddagger}p < 0.01$.

Tissue type	Attenuation (dB/mm/MHz)	Sound speed (m/s)
Normal mucosa	1.04 ± 0.46	1619.4 ± 20.6
Papillary adenocarcinoma	1.12 ± 0.07	1610.0 ± 22.4
Tubular adenocarcinoma		
Well-differentiated	2.12 ± 0.28†	1666.9 ± 16.7†
Moderately-differentiated	1.43 ± 0.10	1600.2 ± 5.0
Poorly-differentiated adenocarcinoma	0.69 ± 0.06†	1556.7 ± 4.1†
Signet-ring cell carcinoma	0.49 ± 0.09‡	1523.3 ± 9.4‡

of the values. In the signet-ring cell carcinoma specimen, the attenuation constant is 0.49 ± 0.09 dB/mm/MHz and the sound speed is 1523.3 ± 9.4 m/s. These values are significantly lower than those of normal tissue (1.06 ± 0.46 dB/mm/MHz, $p < 0.05$ and 1619.4 ± 20.6 m/s, $p < 0.05$, respectively) and other types of gastric cancer tissues except poorly-differentiated adenocarcinoma, for which it can be stated that the attenuation and the sound speed increase as the cellular differentiation of the gastric cancer proceeds.

DISCUSSION

The sound speed of signet-ring cell carcinoma is less than that of normal tissue. Figure 7 shows optical

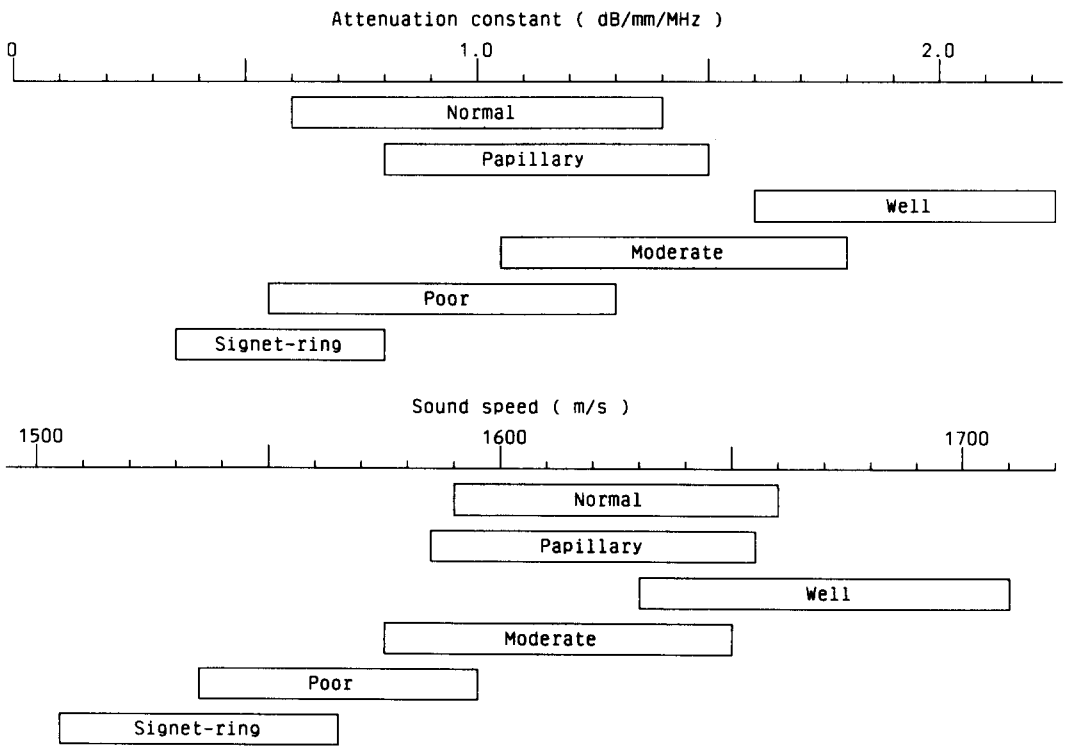

Fig. 6. Graphic illustration of ranges of the attenuation constant and sound speed.

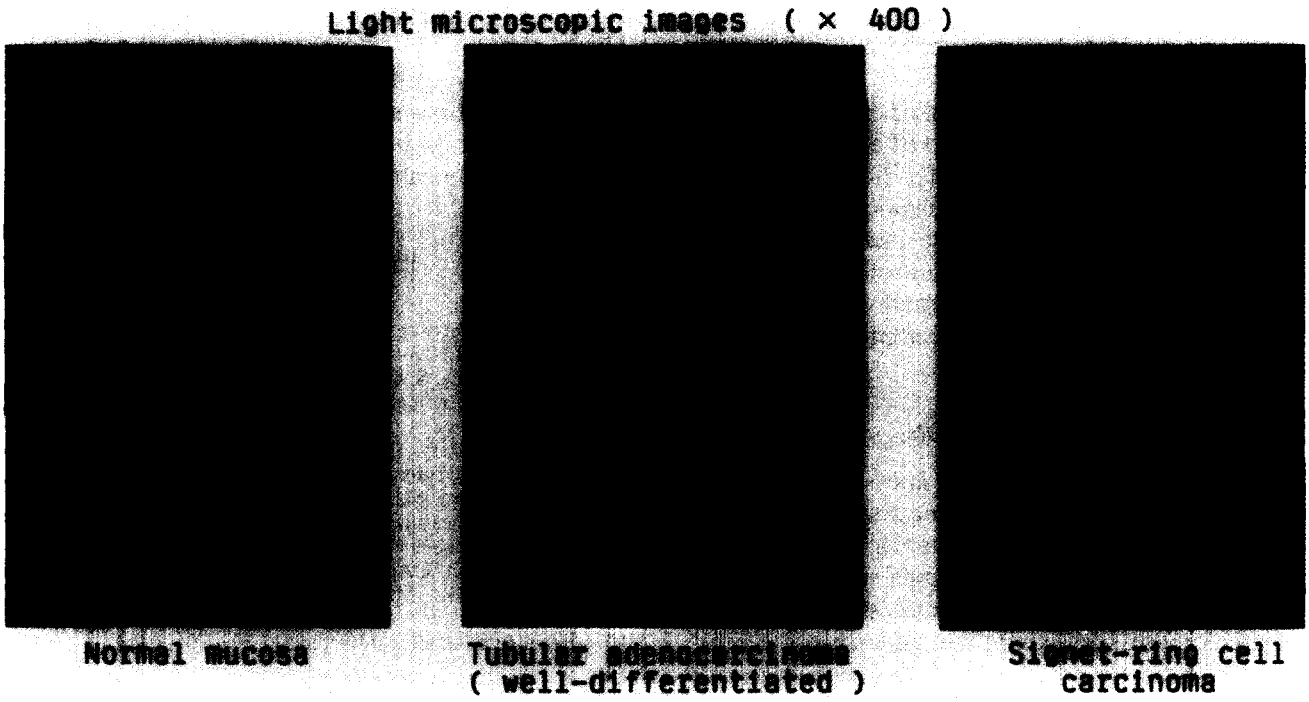

Fig. 7. Light microscopic images of normal mucosa, well-differentiated tubular adenocarcinoma and signet-ring cell carcinoma (H-E staining; ×400).

microphotographs of signet-ring cell carcinoma, well-differentiated tubular adenocarcinoma and normal mucosa. These figures show that the size of the signet-ring cell is larger than that of the normal mucosal tissue and consequently, the number density of signet-ring cells is less than that for normal mucosa. It is also seen that the nucleus/cytoplasm volume ratio in the signet-ring cell is small because the nucleus is forced to the periphery by the periodic acid, Schiff stain (PAS) positive substrate. Electron microscopy shows that the number of desmosomes, which are considered to attach cell-to-cell, is decreased in the signet-ring cell carcinoma (Goldman and Ming 1968; Nevalainen and Jarvi 1977). These factors may combine to produce a reduced bulk elasticity of the tissue in association with the looser cellular junction. This lesser stiffness accounts for reduced sound speed values.

As the SAM operated in the frequency range 100–200 MHz, the resolution was of the order of 10 μm, and it was not possible to determine the acoustic properties of 1–5 μm cells. However, as uniform areas of signet-ring cell carcinoma and of normal tissue were selected for the study, the findings of lesser attenuation and sound speed in signet-ring cell carcinoma tissue reflected the bulk tissue characteristic. A characteristic of signet-ring cells is that they are distended by the abundant mucin. Therefore, the intracellular chemical components may also influence the acoustic properties.

The results of the measurements of tubular adenocarcinoma specimens suggest the tendency that attenuation constant and sound speed become increased as the cell type becomes differentiated. This means that tubular adenocarcinoma tissues become acoustically stiffer as the differentiation of the tissue proceeds. The optical microscopic study showed that the cellular arrangement of poorly-differentiated adenocarcinoma is sparse and disordered. The electron microscopic study showed that the number of desmosomes is significantly decreased in poorly-differentiated adenocarcinoma. Well-differentiated tubular adenocarcinoma specimens exhibit nearly the same number of desmosomes as in normal mucosal tissue, and its polarity is ordered, *viz.*, the nucleus locates near the basement membrane. As the intercellular junction is tight in well-differentiated tubular adenocarcinoma tissue, the well-differentiated tubular adenocarcinoma may be stiffer than the poorly-differentiated adenocarcinoma. These results suggest that gastric cancer tissue is differentiated both histologically and acoustically.

In all types of cancer, and in normal tissue as well, the characteristics leading to high attenuation and fast sound speed are that the cellular distribution is dense and that the cellular arrangement is ordered. The reason high attenuation is considered is that the absorption of ultrasound is very large in such stiff structural tissues. The results of these measurements

show that the structure and three-dimensional arrangement intensely influence the biological acoustic properties of tissue.

Since the specimens were fixed in formalin and embedded in paraffin, the observed attenuation and sound speed values may be greater than that for normal fresh tissues because the mechanical properties of the tissue became stiffer due to increased protein cross linkings. However, under the same set of fixation and measuring conditions, we were able to characterize the acoustic properties of five different types of gastric cancer in a relative manner.

CONCLUSION

The ultrasonic attenuation and sound speed of five different types of gastric cancer specimens were measured. The attenuation constant and sound speed values of signet-ring cell carcinoma specimens were very low compared to normal tissues, and tubular adenocarcinoma tissues exhibit the tendency to become greater than normal tissues as the cell type becomes differentiated.

The data suggest that the ultrasonic properties of gastric cancer tissues are determined, to some extent, by cellular arrangement, intercellular junction and intracellular chemical components.

REFERENCES

DiMango, E. P.; Buxton, J. L.; Regan, P. T. The ultrasonic endoscope. Lancet 1:629–631; 1980.

Goldman, H.; Ming, S. C. Fine structure of intestinal metaplasia and adenocarcinoma of the human stomach. Lab. Invest. 18:203–210; 1968.

Nevalainen, T. J.; Jarvi, O. H. Ultrastructure of intestinal and diffuse type gastric carcinoma. J. Path. 122:129–136; 1977.

Okawai, H.; Tanaka, M.; Chubachi, N.; Junichi, K. Non-contact simultaneous measurement of thickness and acoustic properties of a biological tissue using focused wave in a scanning acoustic microscope. Jpn. J. Appl. Phys. 26:52–54; 1987.

Okawai, H.; Tanaka, M.; Dunn, F.; Chubachi, N.; Honda, K. Quantitative display of acoustic properties of the biological tissue elements. Acoustical Imaging 17:193–201; 1988.